IMPROVEMENT OF CONSPICUITY BY FUSION OF PULSE-ECHO DATA

S. M. Song[1], H. Jang[1], J. Kwon[1], J. Sung[2], H. Ahn[2], J. Lee[2] and S. Jang[2]
[1] Seoul National University, Seoul, Korea;
[2] Sae-An Engineering Corporation, Seoul, Korea

Abstract: Ultrasonic nondestructive testing based on pulse-echo measurements cannot detect faults if there is no reflected energy. Faults that are hidden behind an obstacle (for instance, another fault), or faults angled along the direction of beam propagation reflect negligible energy and will be difficult to detect. Thus, for a thorough examination of 3-D structures, pulse-echo data is collected from the same location using three different incident angles using different wedges attached to the acoustic probe. Typically, the data from the three wedges, for instance, 0-, 45- and 60-degree wedges, are simultaneously collected on three separate channels. The inspector then evaluates the data from all three channels.

In this paper, we present a data fusion approach that strategically "fuses" all collected data to improve conspicuity of faults. Obvious advantages of the proposed data fusion are: (1) to visualize occluded faults (if at least one of channel "sees" the fault), (2) the signal-to-noise ratio (SNR) is expected to improve by the factor $\sqrt{N}$ where N is the number of channels, even by performing a simple averaging as data fusion, and (3) the inspector only has to view one fused data set rather than all the collected data sets.

In particular, the data fusion is applied to the problem of 3-D rendering techniques, namely volume rendering (VR), surface rendering (SR) and maximum intensity projection (MIP). The exact fusion algorithm will differ for different rendering algorithms (SR, VR and MIP) and all will show improved conspicuity for better detection of faults.

Introduction: The goal of nondestructive testing is to detect faults (or discontinuities) inside or outside the structure and to evaluate physical and mechanical characteristics without harming it (Bray, 1997). Of various nondestructive testing methods, the ultrasonic pulse-echo method has proved to be effective, especially for metal structures.

The pulse-echo ultrasonic system usually provides one or all three display formats: A-, B- and C-scan. These displays offer information regarding the nature of the faults, for instance, cracks in metal structures such as pipes and plates. However, only experts trained to interpret A-, B-, or C-scan data is able to detect and locate such faults, especially small miniature cracks. Therefore, to improve conspicuity of faults, we propose a 3-D ultrasonic imaging system based on the pulse-echo measurements to display the data in 3-D, allowing the user to rotate and manipulate the structure. The proposed system gives additional insight since various 3-D views provides additional information that is otherwise unavailable. Furthermore, 3-D views allow users to conveniently locate and measure each faults with greater precision.

Providing 3-D views of human anatomy has recently gained popularity in medical community as more patients are scanned volumetrically (usually acquired as a sequence of slice images). As certain imaging protocols will acquire over 100 slice images, volumetric processing and viewing of such data has become a necessity for providing timely diagnosis of patients. Typically, the volumetric data, *e.g.*, a stack of hundreds of images, is processed by one of the following techniques: surface rendering (SR), volume rendering (VR), and maximum intensity projection (MIP) (Roth, 1982; Robb, 1995). The surface rendering technique first extracts the surface to be visualized (usually by a simple threshold) and then, based on the orientation of the surface, the technique renders the surface according to an artificial light source. The volume rendering techniques are mostly based on ray-casting algorithms (Roth, 1982) that paint each pixels on the display according to the voxel values that lie on the ray. The maximum intensity projection also casts rays but selects the maximum intensity on the ray to be painted on the display. These visualization techniques (SR, VR and MIP) mostly have dealt with magnetic resonance images (MRI) and X-ray computed tomographic (CT) images. As for 3-D visualization of medical images using ultrasonic pulse-echo data, various surfaces have been rendered by detecting the interfaces between two tissue types (Capineri, 1996; Prager, 2002), and several similar techniques show promise for imaging various regions of the anatomy, such as articular cartilage (Lefebvre, 1998), prostate (Tong, 1996), and heart (Salustri, 1995). In this

paper, we propose a 3-D ultrasonic imaging system that collects and processes multiple pulse-echo data in 3-D for visualization and non-destructive evaluation.

We have previously reported some initial results on the MIP technique to visualize the pulse-echo data using MIP (Son, 2002; Song, 2003) as well as the SR and VR (Kwon, 2004). In this paper, we extend our previous results, and propose a technique to fuse the acquired data to improve the conspicuity of faults. Ultrasonic nondestructive testing based on pulse-echo measurements cannot detect faults if there is no reflected energy. Faults that are hidden behind an obstacle (for instance, another fault), or faults angled along the direction of beam propagation reflect negligible energy and will be difficult to detect. Thus, for a thorough examination of 3-D structures, pulse-echo data is collected from the same location using three different incident angles using different wedges attached to the acoustic probe. Typically, the data from the three wedges, for instance, 0-, 45- and 60-degree wedges, are simultaneously collected on three separate channels. The inspector then evaluates the data from all three channels.

In this paper, we present a data fusion approach that strategically "fuses" all collected data to improve conspicuity of faults. Obvious advantages of the proposed data fusion are: (1) to visualize occluded faults (if at least one of channel "sees" the fault), (2) the signal-to-noise ratio (SNR) is expected to improve by the factor $\sqrt{N}$ where N is the number of channels, even by performing a simple averaging as data fusion, and (3) the inspector only has to view one fused data set rather than all the collected data sets. In particular, the data fusion is applied to the problem of 3-D rendering techniques, namely volume rendering (VR), surface rendering (SR) and maximum intensity projection (MIP). The exact fusion algorithm will differ for different rendering algorithms (SR, VR and MIP) and all will show improved conspicuity for better detection of faults.

Data Acquisition and 3-D Visualization: Figure 1 (a) depicts the pulse-echo data acquisition approach. The transducer is placed on top of the specimen and collects the pulse-echo data moving along the raster scan line. For instance, at one scan line, we acquire one B-scan data from the specimen. The entire B-scan data of the specimen is essentially a sequence of slice images for the specimen. These B-scan data pass through the Wiener filter and the linear interpolator before the 3-D visualization step for the generation of 3-D images. For details see (Song, 2003; Kwon, 2004).

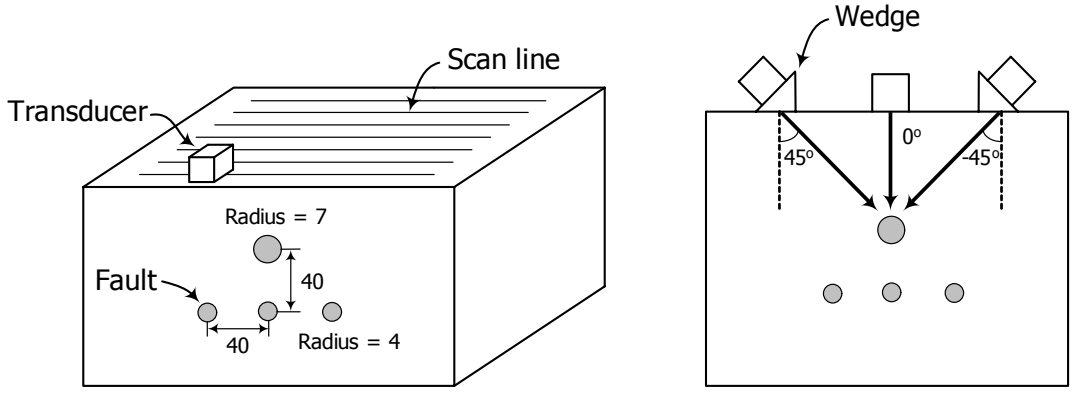

(a) (b)

Fig. 1 The 3-D object and the data acquisition. Units are in millimetres (mm).

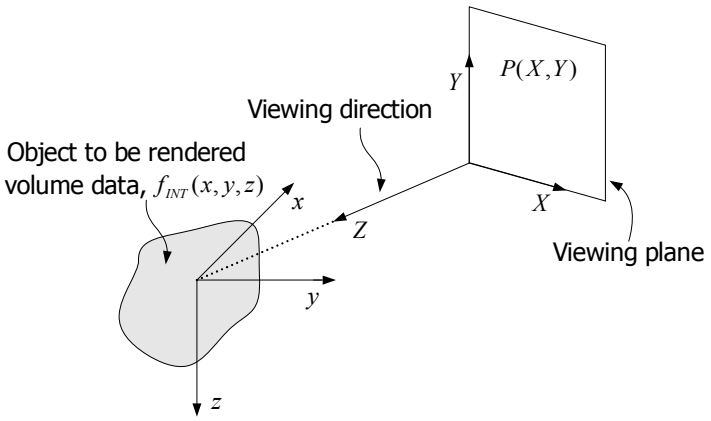

Fig. 2 The relationship between the data acquisition coordinate (x,y,z) and the rotated coordinate (X,Y,Z).

Once all data has been acquired and processed, the data can be visualized using any of the previously discussed 3-D visualization techniques, *i.e.*, surface rendering (SR), volume rendering (VR) and maximum intensity projection (MIP). Figure 2 shows the graphical representation of the 3-D visualization step. The object to be rendered, modelled by the data $f_{INT}(x,y,z)$, is acquired in the (x,y,z) coordinate. For instance, $f_{INT}(x,y,z_0)$ for a fixed z, may represent one B-scan image. The user has the choice of the viewing direction, Z (which may in fact be changed in real-time), and $f_{INT}(x,y,z)$ is to be projected along the direction of Z-axis. Thus, the image data $f_{INT}(x,y,z)$ is first rotated and then projected onto the X-Y plane, resulting in the final image $P(X,Y)$. All three rendering techniques, SR, VR and MIP only differ in the way these rendering techniques compute the projection values. We briefly discuss each technique.

Surface rendering (SR) is the visualization technique that shows the exterior surface of the object. Therefore, before the actual visualization step, SR extracts the exterior surface of the object (Udupa, 1990). In general, surface boundary voxels are determined using a threshold value. Then, the marching cube or marching voxel algorithm is applied to the surface boundary voxels to determine the surface (Lin, 2001).

After the surface extraction, the object is rendered in 3-D using various light sources and their reflections. There are three types of reflection, *i.e.*, diffuse, specular and ambient reflections (Wood, 1992; Tiede, 1990). The ambient reflection is caused by the ambient light source that only depends on the specific environment without a specific direction. Disregarding the specular and ambient terms, the surface rendered image may be stated as:

$$P_{SR}(X,Y) = \mathrm{LUT}[(L(s(X,Y)) \cdot N(s(X,Y))]$$

where $s(X,Y)$ is the "surface element" that would be projected onto the location (X,Y) on the viewing plane. $L(s(X,Y))$ and $N(s(X,Y))$ denote the direction of the light source and the surface normal vector at $s(X,Y)$, respectively. Lastly, LUT is a suitable look-up-table for the color assignment. In general, SR is not suitable for thin and detailed objects (Robb, 1999).

Volume Rendering (VR) uses volume data directly without the surface extraction step of SR (Udupa, 1990). The most distinctive characteristics of VR are opacity and color, determined from the voxel intensities and threshold values. The opacity can have values between zero and unity, which enable rendering of multiple objects simultaneously through transparent effects. The colors of voxels are used to distinguish different objects rendered simultaneously (Levoy, 1988). Mathematically, the rendered image may be stated as:

$$P_{VR}(X,Y) = \sum_{Z=1}^{n} c(f_{INT}(X,Y,Z))\alpha(f_{INT}(X,Y,Z))\prod_{Z'=0}^{Z-1}[1-\alpha(f_{INT}(X,Y,Z'))]$$

where $\alpha(\cdot)$ and $c(\cdot)$ represent opacity and color, respectively. VR is superb for thin and detailed objects, and suitable for transparent effects (Robb, 1999).

Maximum Intensity Projection (MIP) uses the intensity volume data directly without surface extractions or the ad-hoc assignment of opacity and color. The ray traverses the voxels and the maximum voxel value is painted on the viewing plane (Sun, 1999; Schreiner, 1993). The MIP process can be expressed as the following:

$$P_{MIP}(X,Y) = \max_{Z}\{f_{INT}(X,Y,Z)\}$$

As such, MIP is extremely simple to implement and is known to be an effective visualization method especially for vessel structures (Sun, 1999). But, MIP discards the depth information; however, the depth information can be assimilated by showing MIP images at several different angles in a short sequential movie (Schreiner, 1993).

Three-dimensional Visualization by Data Fusion: Suppose we have several 3-D data sets of an identical object. The data set may be acquired several times with different (or even identical) acquisition parameters. In pulse-echo measurements, a structure located "behind" another structure will be hidden and these hidden structures may only become visible using a different wedge attached to the probe (cf. Fig. 1 (b)). Thus, the observer will only be able to locate faults upon viewing all 3-D data sets.

On the other hand, the data may be fused to provide one comprehensive 3-D data set for the observer. The three visualization techniques discussed above (SR, VR and MIP) require different methods of data fusion. In what follows, we propose data fusion techniques for visualization purposes, to "fuse" multiple 3-D data sets of the identical object acquired N times.

Fused Surface Rendering (FSR) paints on the viewing plane, the very first surface visible from (X,Y). As the goal of non-destructive evaluation is to find all faults within the structure, the goal here is to display all surfaces that are present in all acquired data. Denote all surfaces extracted from the N data sets as $s_k(X,Y)$, $k = 1,2,\mathrm{K}\ ,N$. Thus, $s_k(X,Y)$ is the first surface element encountered by the ray originating from (X,Y) for the k^{th} data set. As surface rendering provides depiction of the "first" surface encountered by the ray, here, we merely extend it to multiple data sets. Thus, we use the first surface among all 3-D data sets. Denote $s_0(X,Y)$ as the "first" surface encountered by the ray, *i.e.*, the surface "closest" to (X,Y). Hence, the SR by fusion may be

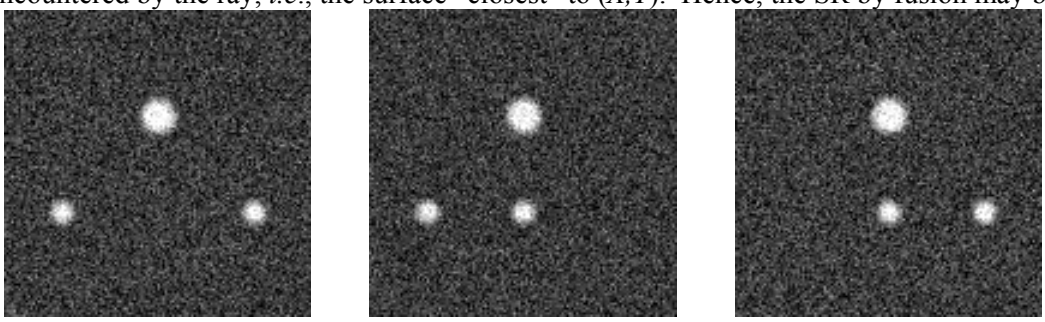

(a) (b) (c)

Fig. 3 A slice of the 3-D data set (*i.e.*, B-scan data) with (a) 0˚ , (b) 45˚ and (c) -45˚ wedges

expressed as:

$$P_{FSR}(X,Y) = \mathrm{LUT}[(L(s_0(X,Y)) \cdot N(s_0(X,Y))]$$

where $s_0(X,Y)$ is the "first" surface among the N data sets.

Fused Volume Rendering (FVR) paints on the viewing plane a strategic combination of opacity and colors. As rays are cast, the individual color is selected and propagated according to opacity values. Suppose individual 3-D data sets are rendered independently. The image resulting from the data fusion should preserve the color. As such, at each position of the ray, we select the maximum intensity (*i.e.*, prominent voxels), color and opacity of this maximum value are propagated. Mathematically it may be expressed as:

$$P_{FVR}(X,Y) = \sum_{Z=1}^{n} c\left(\max_k\left(f_{INT}^k(X,Y,Z)\right)\right)\alpha\left(\max_k\left(f_{INT}^k(X,Y,Z)\right)\right)\prod_{Z'=0}^{Z-1}\left[1-\alpha\left(\max_k\left(f_{INT}^k(X,Y,Z')\right)\right)\right]$$

where $f_{INT}^k(X,Y,Z)$ is the k^{th} 3-D data, and as before, $\alpha(\cdot)$ and $c(\cdot)$ represent the opacity and color, respectively.

Fused Maximum Intensity Projection (FMIP) projects the maximum value onto the viewing plane. The obvious extension to *N* data sets is to paint the maximum value. Thus, mathematically,

$$P_{MIP}(X,Y) = \max_Z\left\{\max_k\left(f_{INT}^k(X,Y,Z)\right)\right\}$$

Results: We present some preliminary results from simulation studies. Figure 1 (a) shows the data acquisition scheme, together with the 3-D object. The three dimensional object (one cylinder with radius 7 mm and three cylinders with radius 4 mm) depicted in Fig. 1 (a) is used for the data generation. Three 3-D data sets are generated with three different wedges as shown in Fig. 1 (b), which we denote -45, 0 and 45 degree wedges. Note that in -45 and 45 degree wedges are physically identical, but differ in the scan direction. Additive Gaussian noise is added (SNR of about 8 dB with respect to the signal reflected by the cylinder) to simulate real noisy measurement environment.

Figure 3 (a), (b) and (c) shows the data acquired using 0, 45 and -45 degree wedges, respectively. The images are essentially one slice of the 3-D volume data, namely the B-scan image. The stack of the three 3-D data sets may be visualized individually or "fused" as discussed previously. We present our results.

Figure 4 (a), (b), (c) and (d) show results of the Surface Rendering. Fig. 4 (a), (b) and (c) are the surface rendered (SR) images using the 0, 45 and -45 degree wedges, respectively. Fig. 4 (d) is the result of the proposed Fused Surface Rendering. Notice that only Fig. 4 (d) depicts all four cylinders.

Similar results are shown for volume rendering as well as maximum intensity projections. These results are summarized in Fig. 5 and Fig. 6 for VR and MIP, respectively.

Discussion and Conclusion: We proposed several data fusion techniques for fusing multiple 3-D data sets for visualizing 3-D structures. We reviewed the existing techniques, namely, surface rendering, volume rendering and maximum intensity projection, and extended these approaches to merge (or fuse) multiple 3-D data sets into one comprehensive 3-D data set. The three visualization techniques, namely surface rendering, volume rendering and maximum intensity projection, popularly used for medical images have all been extended (or generalized) to work with multiple 3-D data sets with the goal of depicting all structures (or faults) present in a 3-D structure. In addition, our preliminary study indicates that each rendering technique has advantages and disadvantages for viewing and detecting various types of faults. For instance, MIP images provide a clear picture of the faults, however, without any depth information. Volume rendered images will be superior for viewing multiple faults, due to its built-in transparency effects, being able to "see-through" a number of overlapping faults. Surface rendered images are probably the best for sizing the detected faults as long as a good surface detection algorithm can be identified. The usefulness of the proposed data fusion technique is the user convenience as it will no longer be required to review multiple 3-D volume data.

Acknowledgment: This research was supported in part by a grant from Sae-An Engineering Corporation.

References:

(Bray, 1997) D. E. Bray and R. K. Stanley, *Nondestructive Evaluation*, CRC Press, New York, 1997.

(Capineri, 1996) L. Capineri, L. Masotti, S. Rocchi, F. andreuccetti, M. Cerofolini and A. Tondini, "Nearly real-time visualization of arbitrary two-dimensional sections from three-dimensional acquisition", *Ultrasound in Med. & Biol*., vol. 22, no. 3, pp. 319-328, 1996.

(Kwon, 2004) J. Kwon, S. M. Song, H. Chang, J. Sung, H. Ahn, J. Lee, and S. Jang, "Generation of three-dimensional images using ultrasonic pulse-echo data for fault characterization", *Key Engineering Materials*, in press (July, 2004)

(Lefebvre, 1998) F. Lefebvre, N. Graillat, E. Cherin, G. Berger and A. Saied, "Automatic three-dimensional reconstruction and characterization of articular cartilage from high-resolution ultrasound acquisitions", *Ultrasound in Med. & Biol*., vol. 24, no. 9, pp. 1369-1381, 1998.

(Levoy, 1988) M. Levoy: "Display of surfaces from volume data", *IEEE Computer Graphics and Applications*, vol. 8, pp. 29-37, 1988.

(Lin, 2001) C. Lin, D. Yang and Y. Chung: "A marching voxels method for surface rendering of volume data" in *Proc. Computer Graphics International 2001*, pp. 306-313, 2001.

(Prager, 2002) R. Prager, A. Gee, G. Treece, and L. Berman, "Freehand 3D ultrasound without voxels: volume measurement and visualization using the Stradx system", *Ultrasonics*, vol. 40, pp. 109-115, 2002

(Robb, 1995) R. A. Robb, *Three-Dimensional Biomedical Imaging*, VCH Publisher Inc., New York, 1995.

(Robb, 1999) R. A. Robb, *Biomedical Imaging, Visualization and Analysis*, Wiley-Liss Inc., New York, 1999.

(Roth, 1982) R. Roth, "Ray casting for solid modeling", *Comput. Graph. Image Proc*., vol. 18, pp. 109-144, 1982.

(Salustri, 1995) A. Salustri and J. Roelandt, "Ultrasonic three-dimensional reconstruction of the heart", *Ultrasound in Med. & Biol*., vol. 21, no. 3, pp. 281-293, 1995.

(Schreiner, 1993) S. Schreiner and R. L. Galloway: "A fast maximum intensity projection algorithm for generating magnetic resonance angiograms"*, IEEE Trans. Med. Img*., vol. 12, no. 1, pp. 50-57, 1993.

(Son, 2002) S. Son, S. M. Song, J. Cho, J. Sung, H. Ahn and J. Lee: "Three-dimensional visualization of ultrasound pulse echo data for nondestructive testing of metal structures", in *Proc. 6th Far-East Conference on Nondestructive Testing*, pp. 159-614, 2002.

(Song, 2003) S. M. Song, S. Son, J. Cho, J. Sung, H. Ahn and S. Jang: "Ultrasonic nondestructive testing by 3-D processing of pulse-echo signal"*, Journal of Nondestructive Evaluation*, submitted.

(Sun, 1999) Y. Sun and D. L. Parker: "Performance analysis of maximum intensity projection algorithm for display of MRA images", *IEEE Trans. Med. Img*., vol. 18, no. 12, pp. 1154-1169, 1999.

(Tiede, 1990) U. Tiede, K. H. Hoehne, M. Bomans, A. Pommert, M. Riemer and G. Wiebecke: "Investigation of medical 3D-rendering algorithms", *IEEE Computer Graphics and Applications*, vol. 10, p. 41-53, 1990.

(Tong, 1996) S. Tong, D. B. Downey, H. Cardinal and A. Fenster, "A three-dimensional ultrasound prostate imaging system", *Ultrasound in Med. & Biol*., vol. 22, no. 6, pp. 735-746, 1996.

(Udupa, 1990) J. K. Udupa and H. Hung: "Surface versus volume rendering: a comparative assessment" in *Proc. the First Conference on Visualization in Biomedical Computing*, pp. 83-91, 1990.

(Wood, 1992) S. L. Wood: "Visualization and modeling of 3-D structures", *IEEE Engineering in Medicine and Biology Magazine*, vol. 11, pp. 72-79, 1992.

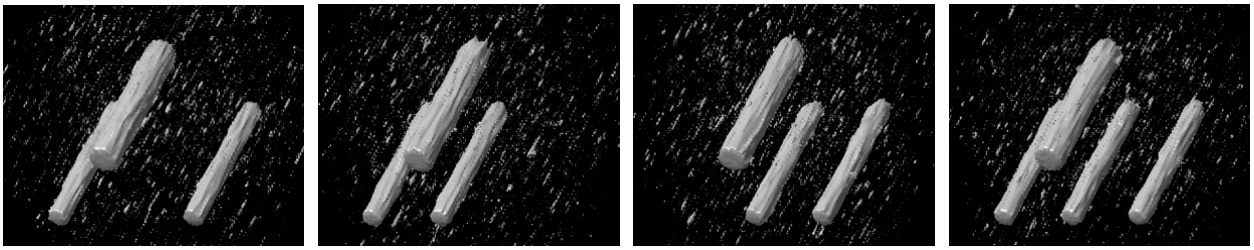

(a) (b) (c) (d)

Fig. 4 Surface rendered images. Individually rendered images, acquired with (a) 0˚, (b) 45˚, and (c) -45˚ wedges, and (d) the "fused" image

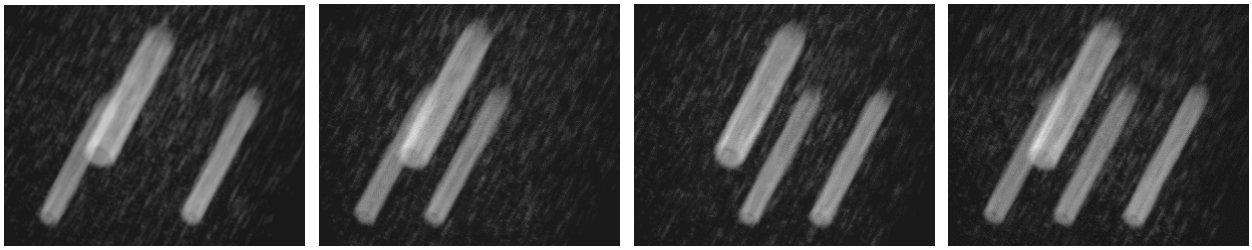

(a) (b) (c) (d)

Fig. 5 Volume rendered images. Individually rendered images, acquired with (a) 0˚, (b) 45˚, and (c) -45˚ wedges, and (d) the "fused" image.

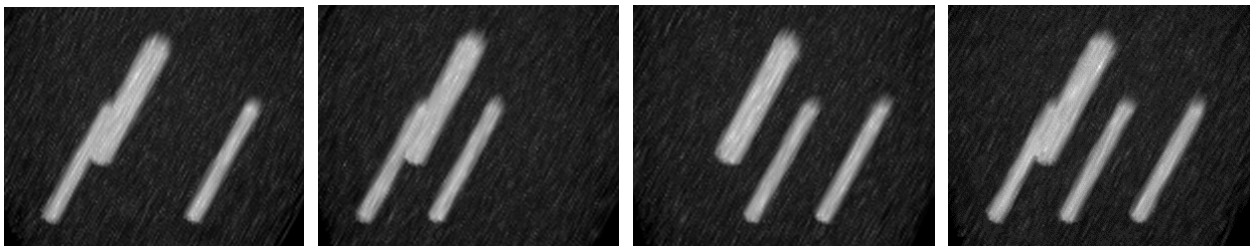

(a) (b) (c) (d)

Fig. 6 Maximum intensity projection images. Individually rendered images, acquired with (a) 0˚, (b) 45˚, and (c) -45˚ wedges, and (d) the "fused" image.